GEOLOGY | THE GEOLOGICAL SOCIETY OF AMERICA®

https://doi.org/10.1130/G49303.1

Manuscript received 22 May 2021
Revised manuscript received 9 August 2021
Manuscript accepted 11 August 2021

Published online 20 October 2021

Polychromatic polarization: Boosting the capabilities of the good old petrographic microscope

Bernardo Cesare[1]*, Nicola Campomenosi[2,3] and Michael Shribak[4]*
[1]Department of Geosciences, University of Padova, via G. Gradenigo 6, 35131 Padua, Italy
[2]Department of Earth Science, Environment & Life, University of Genova, Corso Europa 26, I-16132 Genoa, Italy
[3]Department of Earth Sciences, University of Hamburg, Grindelallee 48, D-20146 Hamburg, Germany
[4]Marine Biological Laboratory, 7 MBL Street, Woods Hole, Massachusetts 02543, USA

ABSTRACT

Polychromatic polarizing microscopy (PPM) is a new optical technique that allows for the inspection of materials with low birefringence, which produces retardance between 1 nm and 300 nm. In this region, where minerals display interference colors in the near-black to gray scale and where observations by conventional microscopy are limited or hampered, PPM produces a full spectrum color palette in which the hue depends on orientation of the slow axis. We applied PPM to ordinary 30 µm rock thin sections, with particular interest in the subtle birefringence of garnet due both to non-isotropic growth or to strain induced by external stresses or inclusions. The PPM produces striking, colorful images that highlight various types of microstructures that are virtually undetectable by conventional polarizing microscopy. PPM opens new avenues for microstructural analysis of geological materials. The direct detection and imaging of microstructures will provide a fast, non-destructive, and inexpensive alternative (or complement) to time-consuming and more costly scanning electron microscope–based analyses such as electron backscatter diffraction. This powerful imaging method provides a quick and better texturally constrained basis for locating targets for cutting-edge applications such as focused ion beam-transmission electron microscopy or atom probe tomography.

INTRODUCTION

The polarizing microscope is the fundamental analytical tool for any first characterization of geological materials. Invented almost two centuries ago (Davidson, 2010), its fundamental structure and analytical capabilities have not changed much since. Due to such long, established use, geologists may not realize that polarizing microscopy suffers from one major limitation, which is namely the poor capability to resolve microstructures where minerals have low birefringence (<0.010) and display interference colors in the gray scale. This corresponds to the range of retardance from 0 to ~300 nm. Many important rock-forming minerals (e.g., feldspars, silica polymorphs, hydrogarnets, andradite, leucite, and apatite) possess such low birefringence intrinsically (Deer at al., 2013). Others, originally cubic, may acquire subtle anisotropy and birefringence due to imposed deformation. One classic example is birefringence haloes around inclusions trapped in diamond (Howell et al., 2010) or garnet (Campomenosi et al., 2020). Techniques to highlight the optical effects of very low birefringence materials include using compensators such as the Bräce-Köhler or the lambda plate. As the retardance is a function of thickness, another way to enhance birefringence effects is to make thicker sections. Although in some cases thick (e.g., 100 µm), sections provide satisfactory results (Cesare et al., 2019), they are seldom used because of the great drop in transparency and sharpness of the subjects imaged.

The above shortcomings of conventional optical microscopy, until now accepted as intrinsic and unsolvable, are overcome by a technique called polychromatic polarizing microscopy (PPM). We show how PPM, implemented as a complementary accessory on petrographic microscopes, allows unprecedented imaging of microstructures in very low birefringence minerals using standard 30 µm thin sections. PPM not only produces a full palette of colors in areas normally dominated by gray, but it allows fast, qualitative determination of crystallographic and strain orientations.

POLYCHROMATIC POLARIZING MICROSCOPY

PPM was first presented as a means of imaging biological objects with birefringence down to a few nanometers. Details of various optical setups and theoretical bases of PPM are given by Shribak (2015, 2017) and provided in the Supplemental Material[1]. The polychromatic polscope is very similar to the petrographic microscope, but the polarizer is accompanied by a special spectral polarization state generator, and the analyzer is accompanied by an achromatic quarter-wave plate, which forms the circular analyzer (Shribak, 1986). This setup makes it easy to switch from PPM to plane-polarized light (PPL) to cross-polarized light (XPL) visualization. Even at very low retardance, PPM produces the full hue-saturation-brightness (HSB) color spectrum in birefringent materials. Unlike in conventional polarizing microscopy, where interference colors are a measure of the retardance according to the Michel-Levy chart, HSB hues in PPM depend on the orientation of the slow vibration direction with respect to a preset zero direction (conventionally oriented E-W). This implies that hues change continuously during the rotation of the stage, repeating every 180°, and that extinction is never observed. For some aspects, PPM recalls the "fabric analyzer" (Wilson et al., 2003), which also uses the orientation of the optical indicatrix to find crystal orientation but requires an ad hoc

*E-mails: bernardo.cesare@unipd.it; mshribak@mbl.edu

[1]Supplemental Material. Description of the polychromatic polarizing microscope. Please visit https://doi.org/10.1130/GEOL.S.16725451 to access the supplemental material, and contact editing@geosociety.org with any questions.

CITATION: Cesare, B., Campomenosi, N., and Shribak, M., 2022, Polychromatic polarization: Boosting the capabilities of the good old petrographic microscope: Geology, v. 50, p. 137–141, https://doi.org/10.1130/G49303.1

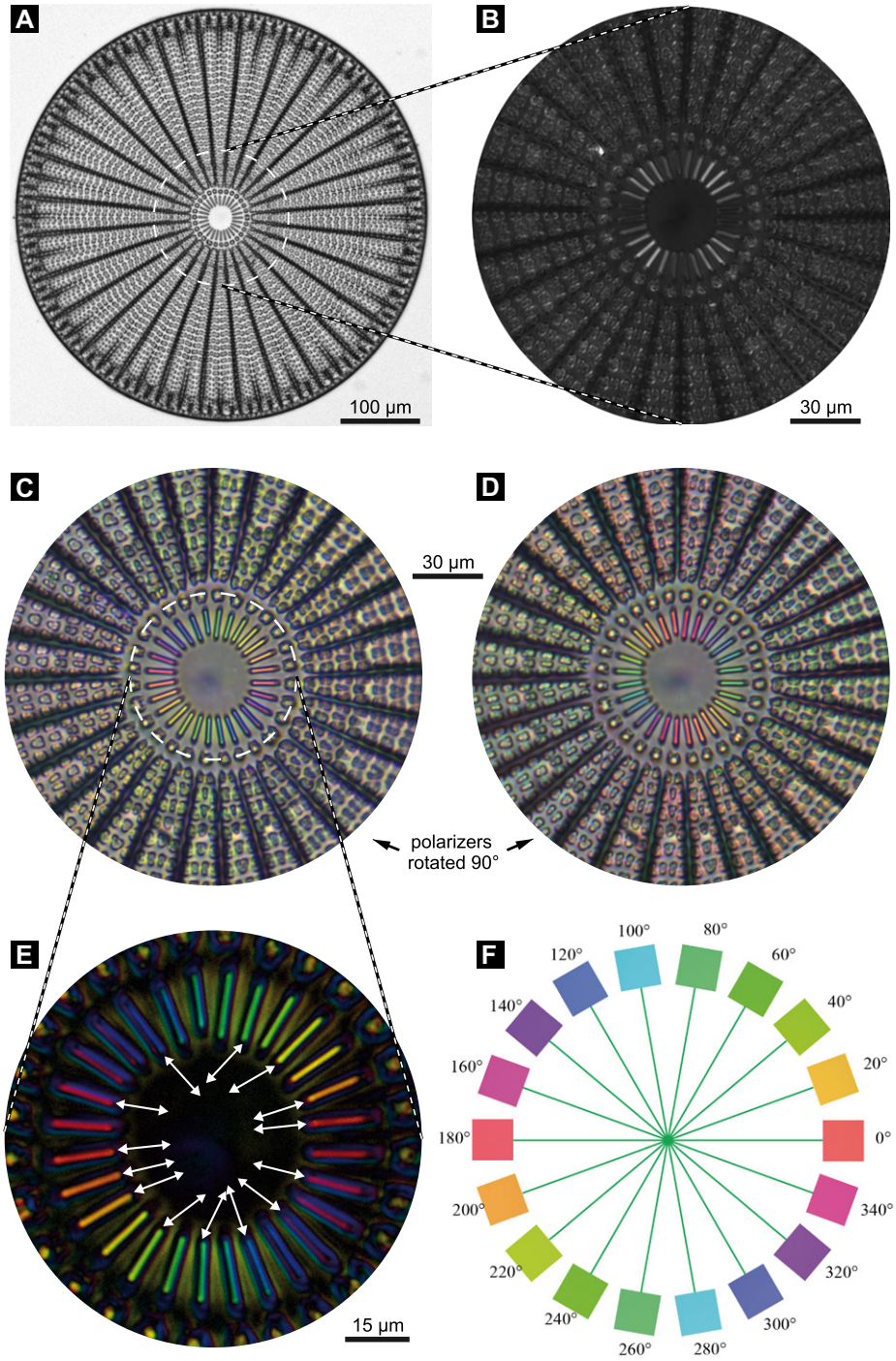

Figure 1. (A) Bright field image showing the siliceous frustule of the diatom *Arachnoidiscus* spp. (B) Cross-polarized light (XPL) detail of the central part of the frustule. (C,D) Two complementary polychromatic polarizing microscopy (PPM) photomicrographs of the same area as in part B taken with polarizers rotated 90° with respect to each other. (E) Detail of the differential image obtained from C and D. Hues of costae in E are the same as in C but more vivid. White arrows indicate the slow vibration direction of each costa to which they point. (F) Calibrated "wheel" of hue variation as a function of optical orientation of a substance. The angular values correspond to the orientation of slow vibration direction with respect to the zero position set as horizontal. Additional details are provided in the Supplemental Material (see footnote 1).

instrument and has never been used on minerals with birefringence of < 0.009.

The functioning peculiarities and potentials of PPM are illustrated by the close-up views on the central part of a frustule of the diatom *Arachnoidiscus* spp. (Fig. 1). These siliceous skeletons are normally black to dark gray under XPL (Fig. 1B). PPM (Fig. 1C) uses colors to visualize the structure of the frustule. By taking a complementary image with the PPM rotated to 90° (Fig. 1D), a differential image can be computed (Fig. 1E), which suppresses the imperfections and provides better measurements of hues. The range and geometric distribution of hues in the inner costae of the diatom are virtually identical to those of the color scheme in Figure 1F, which displays the experimentally calibrated variation of hue as a function of the angle between the slow direction of the birefringent material and the zero position of PPM (E-W in Fig. 1F). Through such analogy, PPM allows us to infer that (1) each of the 28 inner costae (Ross and Sims, 1972) radiating around a central ring of the diatom is a single crystal; (2) costae may be crystalline and not amorphous as commonly thought (e.g., Javaheri et al., 2015; Aitken et al., 2016); (3) they are crystallographically oriented following a radial pattern; and (4) they are length-slow, as the slow vibration direction is parallel to the elongation of each costa (Fig. 1E). Obtaining such a wealth of information on the basis of two optical images alone highlights the exceptional added value of PPM as a novel imaging technique over conventional polarized microscopy.

NON-ISOTROPIC GARNET GROWTH

We tested PPM on common (Fe-Mg-Ca-Mn) tetragonal garnets, which were recently shown to be more common than previously thought (Cesare et al., 2019). They are easily overlooked due to their very low birefringence except when observed in thick (≥100 µm) sections.

On regular 30 µm thin sections of pelites from the eastern Alps, PPM produces striking differential images in areas where XPL would show nothing but apparent isotropy (Figs. 2A–2C). The garnet is unexpectedly optically anisotropic and shows beautiful optical sector zoning with pairs of opposed sectors characterized by similar hue and therefore by similar optical orientation. It should be kept in mind that PPM is a semiquantitative technique, as the direction of the slow vibration axis provided by the hue in PPM images is not absolute but is the direction of the projection of the axis onto the plane of the thin section regardless of the actual dip angle of the axis. The boundaries between adjacent sectors range from sharp and straight to diffuse or compenetrated. Owing to the 30 µm thickness of the samples, these microstructures are much better resolved than when thicker sections are used. PPM was applied (Fig. 2D) to an eclogite from Port Macquarie, Australia (Tamblyn et al. 2019, 2020), that contains garnet compositions in the range expected by Cesare et al. (2019) for non-isotropic garnets. PPM reveals that the garnet crystals are birefringent and beautifully sector-zoned, where different zones may represent growth twins. Being the only technique by which these microstructures can be visualized on regular thin sections, PPM would be a key tool for precisely locating the targets for a focused ion beam (FIB)-based, high-resolution transmission

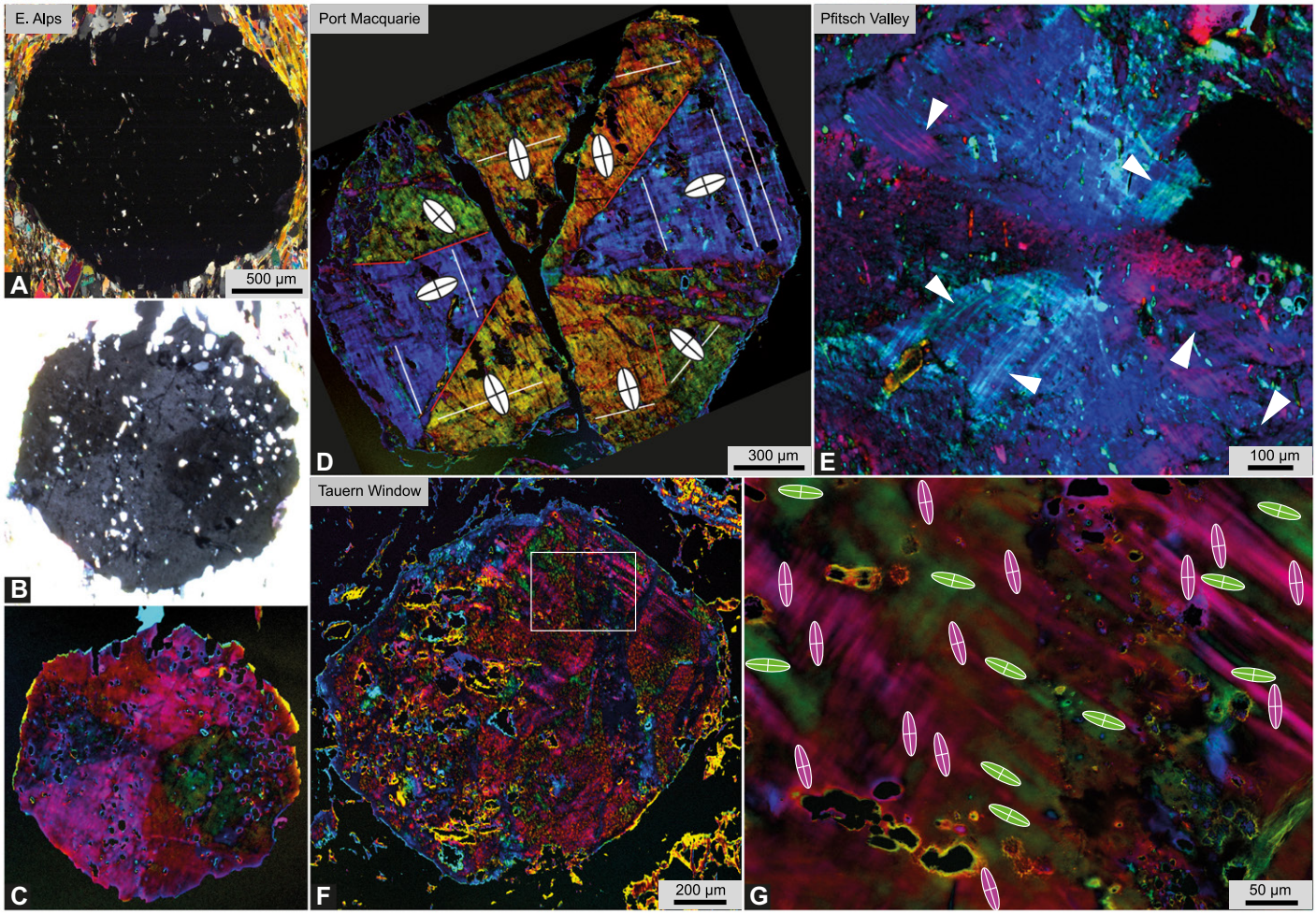

Figure 2. Non-isotropic garnet in 30 µm thin sections. (A–C) Optically sector-zoned garnet from the eastern Alps viewed under (A) cross-polarized light (XPL) with (B) the Bräce-Köhler compensator and (C) with differential polychromatic polarizing microscopy (PPM). (D) Differential PPM image of a garnet from Port Macquarie, Australia. White ellipses indicate the orientations of fast and slow vibration directions, respectively; white lines are traces identifying progressive growth of crystal facets; red lines are sector boundaries. (E) Striped pattern (white arrows) of hue distribution in a garnet of a graphitic schist from the Pfitsch Valley, Italy (Cesare et al., 2019). (F) Differential PPM image of garnet in an eclogite from the Tauern Window (Austria). This garnet displays a diffuse mottled distribution of hue. White box locates the area enlarged in part G. (G) The non-isotropic garnet displays two main optical orientations, reported as green and purple ellipses, at a high angle to each other.

electron microscopy study of possible twinning and its origin. The differential PPM images of Figure 2 also demonstrate, as one would expect, that the optical orientation of sectors is not random. In fact, the fast vibration direction is normal to the growing faces (Fig. 2D).

Optical anisotropy of garnet is also manifested as striped (or mottled) areas of crystals, sometimes within each sector, which is therefore not a coherent optical entity. The parallel stripes or bands can be as thin as a few tens of micrometers and often form intersecting sets characterized by two prevailing optical orientations (Fig. 2E). Striped birefringence patterns are well-developed (Figs. 2F and 2G) in another eclogite sample from the central Tauern Window, Austria (Warren et al., 2012), where, conversely, sector zoning is not evident. Analysis of PPM hue distribution in one of these zones (Fig. 2G) shows that the optic axes of stripes are systematically arranged along two orientations at a high angle to each other.

STRESS-INDUCED BIREFRINGENCE IN GARNET

Another application of PPM concerns the very low birefringence induced by non-isotropic stress fields applied to optically isotropic crystals. Such stress fields may have led to permanent deformation (i.e., plasticity) in the past or may be the signal of an elastic residual stress that is still acting on a crystal at room conditions, for example around inclusions.

Garnet may display crystal plasticity when deformed at high temperature (Prior et al., 2000) and/or high differential stress (Austrheim et al., 2017). Distortion of the crystal lattice may determine an optical anisotropy that is seldom detectable under conventional XPL. Using PPM, we imaged (Figs. 3A–3E) a felsic mylonite from the Musgrave Ranges, central Australia, where garnet underwent both brittle and plastic deformation as determined by electron backscatter diffraction (EBSD) and focused ion beam-transmission electron microscope investigation (Hawemann et al., 2019). The PPM images demonstrate that the complex internal deformation of garnet can also be rendered optically. With diffuse microfracturing along subparallel sets, the variations of hue in the garnet portions bounded by fractures indicate that the entire crystal is affected by crystal plasticity (Fig. 3A). The distribution of hue in the close-up images (Figs. 3B–3D) suggests the presence of a patterned optical orientation of deformed garnet structures. Furthermore, analysis of hue distribution with image processing software like ImageJ (Schneider et al., 2012) highlights the presence of subdomains with sizes in the range of 2–5 µm that display distinct optical orientation with respect to surrounding domains (Fig. 3E). This texture is strikingly similar to that of the subgrains of garnet imaged by EBSD by Austrheim et al. (2017). At present, it is unclear if the hue distribution in these differential PPM images at

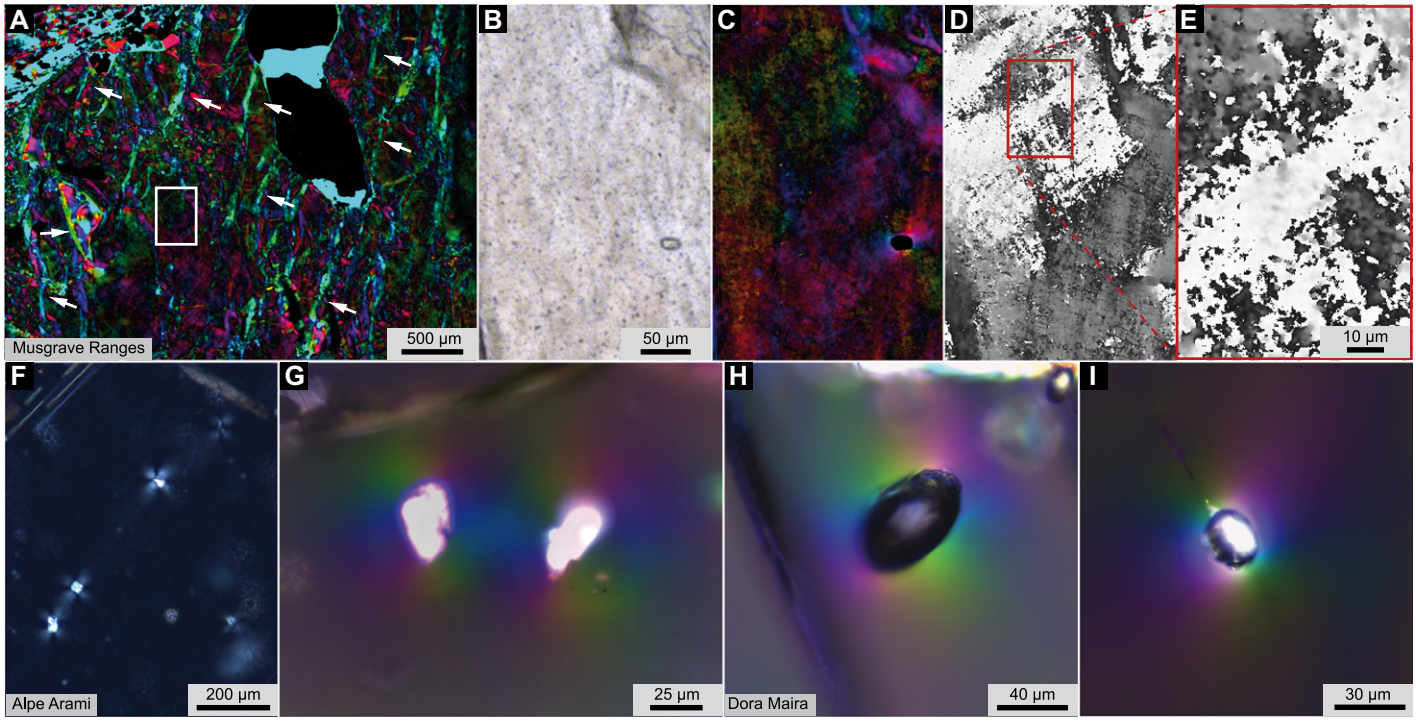

Figure 3. (A–E) Mylonite from the Musgrave Ranges in central Australia. (A) Differential polychromatic polarizing microscopy (PPM) image of a garnet porphyroclast highlighting a subvertical pattern of brittle fractures (arrows). The garnet among fractures is optically anisotropic. (B–D) Plane-polarized light (PPL), PPM, and gray scale views of the garnet area in the white box in part A. Although the PPL micrograph (B) shows microstructures only on the top right corner, the differential PPM (C) shows the ductile strain of garnet through the continuous changes of hue. (D) Gray scale (0, 255) hue map obtained with ImageJ software (https://imagej.nih.gov/ij/index.html). (E) Gray scale detail of the red box in part D shows 2–4-µm-wide areas with similar hues. (F–I) Birefringence halos around inclusions. (F) Cross-polarized light (XPL) image of amphibole inclusions in a garnet from Alpe Arami, Switzerland, shows the cross-shaped extinction pattern. (G) PPM view of two inclusions in the same garnet. (H,I) PPM micrographs of rutile (H) and zircon (I) in a garnet from Dora Maira (western Alps, Italy) whiteschists. The distribution of hues indicates that in all three cases, the slow vibration direction is tangential to inclusions.

high magnification may be affected by optical artifacts and therefore does not correspond to real optical inhomogeneities. Should it, conversely, be verified by further investigation, the possibility of imaging subgrains in garnet optically by PPM would represent a major breakthrough for microstructural analysis.

Lattice strain and anomalous birefringence in optically isotropic minerals is also induced by inclusions trapped at high pressure-temperature during metamorphism due to the contrast of their thermoelastic properties with those of the surrounding host (e.g., Howell et al., 2010). The residual stresses and strains recorded by host-inclusion systems are central to elastic thermobarometry (e.g., Bonazzi et al., 2019). With cooling and exhumation, inclusions typically induce "birefringence halos" in the surrounding garnet host at ambient pressure-temperature conditions. Although these halos are visible under XPL in the form of a cross-shaped extinction pattern (Fig. 3F; Campomenosi et al., 2020), their imaging by PPM reveals important additional features. First of all, the black cross, unavoidable but also of little utility, is not present anymore. Conversely, the entire spectrum of hues covering all possible slow axis orientations is observed around inclusions (Figs. 3G–3I). This provides, without the need to rotate the stage and sample, immediate visualization of the continuous change of orientation of optic axes in the garnet that is now locally anisotropic. Such qualitative visualization can be refined by inspection of hue distribution by which, for example, departures from a purely radial pattern due to the shape and intrinsic anisotropy of mineral inclusions can be detected and analyzed (Fig. S1 in the Supplemental Material).

PERSPECTIVES

Although we focused our attention on garnet, the applications of PPM in the geosciences extend to all materials that possess very low retardance. For example, the unprecedented visualization of microstructures of *Arachnoidiscus* spp. (Fig. 1) demonstrates the potential that PPM has for the study of siliceous microfossils. The best applications of PPM are probably yet to be discovered. We foresee that PPM will become a fundamental tool for studying microstructures in crystals that—from the view point of the optical properties—are nominally isotropic or intrinsically birefringent (Burnett et al., 2001) or show low birefringence such as, for example, leucite, feldspars, and silica polymorphs (Fig. 4).

The imaging capabilities of PPM, especially in differential mode, disclose a wealth of microstructural features that until now were optically inaccessible. PPM can be accomplished using a standard petrographic microscope and conventional thin sections, thus making PPM a fast and extremely cost-effective technique. Among the newest and most important utilities of PPM is the easy identification of the optical orientation of a (portion of) crystal by means of its hue such as, for example, the chalcedony fibers in Figures 4C and 4D. Although this is a semiquantitative method that cannot replace quantitative approaches such as universal stage or EBSD, the applications on garnet described above show that PPM is the perfect tool, and far more precise than conventional polarizing microscopy, for identifying and localizing targets for advanced analyses like TEM or atom probe tomography.

ACKNOWLEDGMENTS

We thank J. Faithfull, R.D. Law, and C. Passchier for their reviews; M. Hand, G. Pennacchioni, R. Tamblyn, and C. Warren for kindly providing samples imaged by polychromatic polarizing microscopy; and M. Alvaro for discussion. We acknowledge the financial support of the Italian Ministry of Education, University and Research-Research Projects of National Relevance grant 2017ZE49E7 to B. Cesare, the National Institute of General Medical Sciences/National Institutes of Health grant R01-GM101701 to M. Shribak, and the Alexander von Humboldt Foundation (Bonn, Germany) to N. Campomenosi.

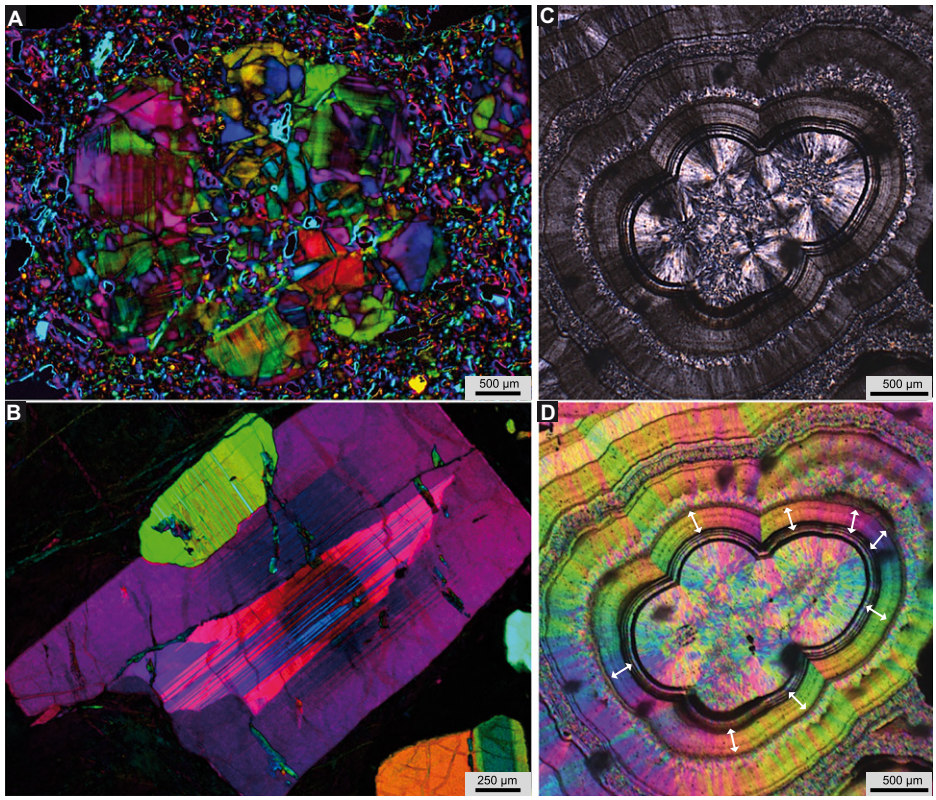

Figure 4. (A) Differential polychromatic polarizing microscopy (PPM) image of a porphyritic lava from Vesuvius, Italy. The leucite in the center of view forms a glomerocryst consisting of numerous twinned crystals that are distinguishable by the distribution of hues. (B) Differential PPM photomicrograph of a plagioclase phenocryst. The resorbed core and the concentric zoning are easily identified by the sudden and continuous changes of hue, respectively. (C,D) Cross-polarized light (XPL) and PPM photomicrographs of a banded agate. With a single colorful image, PPM allows fast identification of the optical orientation of chalcedony fibers. Fast vibration directions (white arrows) indicate that this chalcedony is length-fast.

REFERENCES CITED

Aitken, Z.H., Luo, S., Reynolds, S.N., Thaulow, C., and Greer, J., 2016, Microstructure provides insights into evolutionary design and resilience of ***Coscinodiscus*** sp. Frustule: Proceedings of the National Academy of Sciences of the United States of America, v. 113, p. 2017–2022, https://doi.org/10.1073/pnas.1519790113.

Austrheim, H., Dunkel, K.G., Plümper, O., Illefonse, B., Liu, Y., and Jamtveit, B., 2017, Fragmentation of wall rock garnets during deep crustal earthquakes: Science Advances, v. 3, e1602067, https://doi.org/10.1126/sciadv.1602067.

Bonazzi, M., Tumiati, S., Thomas, J.B., Angel, R.J., and Alvaro, M., 2019, Assessment of the reliability of elastic geobarometry with quartz inclusions: Lithos, v. 350–351, 105201, https://doi.org/10.1016/j.lithos.2019.105201.

Burnett, J.H., Levine, Z.H., and Shirley, E.L., 2001, Intrinsic birefringence in calcium fluoride and barium fluoride: Physical Review B, v. 64, 241102, https://doi.org/10.1103/PhysRevB.64.241102.

Campomenosi, N., Mazzucchelli, M.L., Mihailova, B.D., Angel, R.J., and Alvaro, M., 2020, Using polarized Raman spectroscopy to study the stress gradient in mineral systems with anomalous birefringence: Contributions to Mineralogy and Petrology, v. 175, p. 1–16, https://doi.org/10.1007/s00410-019-1651-x.

Cesare, B., Nestola, F., Johnson, T., Mugnaioli, E., Della Ventura, G., Peruzzo, L., Bartoli, O., Viti, C., and Erickson, T., 2019, Garnet, the archetypal cubic mineral, grows tetragonal: Scientific Reports, v. 9, p. 1–13, https://doi.org/10.1038/s41598-019-51214-9.

Davidson, M.W., 2010, Pioneers in optics: Giovanni Battista Amici and Girolamo Cardano: Microscopy Today, v. 18, p. 50–52, https://doi.org/10.1017/S1551929510000295.

Deer, W.A., Howie, R.A., and Zussman, J., 2013, An Introduction to the Rock Forming Minerals (third edition): London, The Mineralogical Society, 498 p.

Hawemann, F., Mancktelow, N., Wex, S., Pennacchioni, G., and Camacho, A., 2019, Fracturing and crystal plastic behaviour of garnet under seismic stress in the dry lower continental crust (Musgrave Ranges, Central Australia): Solid Earth, v. 10, p. 1635–1649, https://doi.org/10.5194/se-10-1635-2019.

Howell, D., Wood, I.G., Dobson, D.P., Jones, A.P., Nasdala, L., and Harris, J.W., 2010, Quantifying strain birefringence halos around inclusions in diamond: Contributions to Mineralogy and Petrology, v. 160, p. 705–717, https://doi.org/10.1007/s00410-010-0503-5.

Javaheri, N., Dries, R., Burson, A., Stal, L.J., Sloot, P.M.A., and Kaandorp, J.A., 2015, Temperature affects the silicate morphology in a diatom: Scientific Reports, v. 5, 11652, https://doi.org/10.1038/srep11652.

Prior, D.J., Wheeler, J., Brenker, F.E., Harte, B., and Matthews, M., 2000, Crystal plasticity of natural garnet: New microstructural evidence: Geology, v. 28, p. 1003–1006, https://doi.org/10.1130/0091-7613(2000)28<1003:CPONGN>2.0.CO;2.

Ross, R., and Sims, P.A., 1972, The fine structure of the frustule in centric diatoms: A suggested terminology: British Phycological Journal, v. 7, p. 139–163, https://doi.org/10.1080/00071617200650171.

Schneider, C.A., Rasband, W.S., and Eliceiri, K.W., 2012, NIH Image to ImageJ: 25 years of image analysis: Nature Methods, v. 9, p. 671–675, https://doi.org/10.1038/nmeth.2089.

Shribak, M., 1986, Use of gyrotropic birefringent plate as quarter-wave plate: Soviet Journal of Optical Technology, v. 53, p. 443–446.

Shribak, M., 2015, Polychromatic polarization microscope: Bringing colors to a colorless world: Scientific Reports, v. 5, 17340, https://doi.org/10.1038/srep17340.

Shribak, M., 2017, Polychromatic polarization state generator and its application for real-time birefringence imaging: US Patent 9625369, International Class G01N 21/23.

Tamblyn, R., Hand, M., Kelsey, D., Anczkiewicz, R., and Och, D., 2019, Subduction and accumulation of lawsonite eclogite and garnet blueschist in eastern Australia: Journal of Metamorphic Geology, v. 38, p. 157–182, https://doi.org/10.1111/jmg.12516.

Tamblyn, R., Hand, M., Morrissey, L., Zack, T., Phillips, G., and Och, D., 2020, Resubduction of lawsonite eclogite within a serpentinite-filled subduction channel: Contributions to Mineralogy and Petrology, v. 175, 74, https://doi.org/10.1007/s00410-020-01712-1.

Warren, C.J., Smye, A.J., Kelley, S.P., and Sherlock, S.C., 2012, Using white mica $^{40}Ar/^{39}Ar$ data as a tracer for fluid flow and permeability under high-P conditions: Tauern Window, Eastern Alps: Journal of Metamorphic Geology, v. 30, p. 63–80, https://doi.org/10.1111/j.1525-1314.2011.00956.x.

Wilson, C.J.L., Russell-Head, D.S., and Sim, H.M., 2003, The application of an automated fabric analyzer system to the textural evolution of folded ice layers in shear zones: Annals of Glaciology, v. 37, p. 7–17, https://doi.org/10.3189/172756403781815401.

Printed in USA